Optimal Filler Sizes for Thermal Interface Materials

Piyas Chowdhury *, Kamal Sikka, Alfred Grill, Dishit P. Parekh
IBM Research
257 Fuller Rd
Albany, NY 12203, USA
* Corresponding author: piyas.chowdhury@ibm.com

ABSTRACT

The principal challenge in developing a new thermal interface material (TIM) is to co-design its micro-attributes (e.g. filler type, packing fraction, size distribution) that simultaneously ensure high effective thermal conductivity (k_{eff}), low elastic modulus (E_{eff}) and low viscosity (η_{eff}). Today there exists little physical insight into size distributions of fillers that would optimize desired properties. These thermo-mechanical metrics follow contradicting trends if filler content is only monotonically increased. In this paper, we elucidate microstructure-property correlations vital for optimizing effective properties. First, we systematically vary filler size distributions and generate different particulate structures with a previously developed packing algorithm [1]. Then, we employ mechanistic models, based upon physics of micro-scale heat/force transport, to predict k_{eff}, E_{eff} and η_{eff} of the particulate structure, thereby identifying filler size domains that optimize the desired properties.

KEY WORDS: Packing Algorithm, Thermal Conductivity, Elastic Modulus, Viscosity, Filler Size Distributions

NOMENCLATURE

A	area (m^2)
E	elastic modulus (MPa)
F	force flux (N)
h	particle surface-to-surface distance (m)
k	thermal conductivity (W/m°C)
L	TIM bond line thickness (m)
N	total number of particles
P	probability density function
Q	heat flux (W)
R	thermal resistance (°C/W)
r	radius of particle (m)
T	temperature (°C)
u	displacement (m)

Greek symbols

α	heat/force transfer parameter
η	viscosity (Pa.s)
ε	connectivity parameter
ϕ	volume fraction (%)
Φ	maximum volume fraction achievable (%)
μ	mean particle diameter (m)
σ	standard deviation of particle diameter (m)

Subscripts

i, j	particle index
m, p	matrix, particle
eff	effective
max	maximum

BACKGROUND

In an electronic package, the TIM resides between a heat generating chip and a heat spreader or sink and consists of metallic and non-metallic filler particles dispersed in a polymer matrix (Fig. 1) [2][3][4].

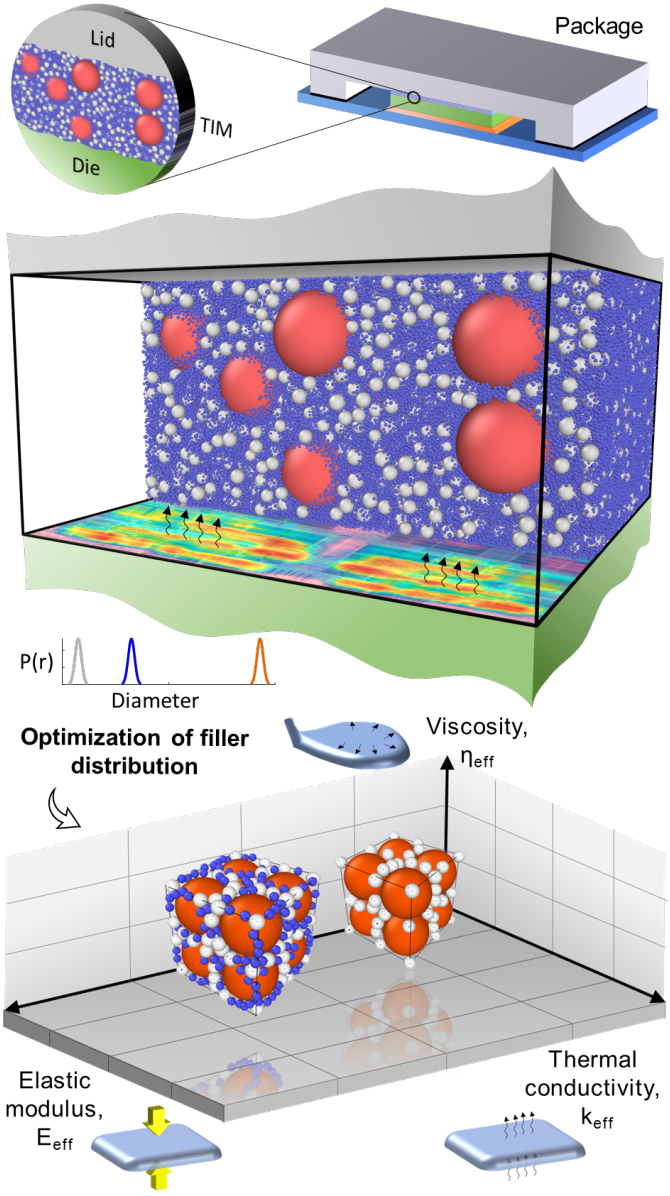

Fig. 1 (Top) Thermal interface material between silicon die and lid. (Middle) heat dissipating non-uniformly from the die to the lid through particulate TIM structure. (Bottom) Current research proposes a method to optimize TIM filler size distributions to achieve desired k_{eff}, E_{eff} and η_{eff} levels.

The heat dissipation from the chip is spatially non-uniform with higher density near the computing cores. The filler particles are provided in different size distributions. In view of improved performance, long-term reliability and ease of assembly, desired thermo-mechanical properties of these oil/filler composite materials are threefold: (a) high thermal conductivity (k_{eff}), (b) low elastic modulus (E_{eff}) and (c) low viscosity (η_{eff}).

High k_{eff} enables higher power dissipation, low E_{eff} ensures small deformation originating from thermal expansion mismatch among components, and low η_{eff} provides better TIM dispensability during package assembly. Currently, formulation of new TIMs with superior properties is a highly challenging task given the trial-and-error based practice of mixing materials. One rule of thumb, for instance, is to pack conductive particles to the maximum density possible into the polymeric matrix. This strategy generally results in increased k_{eff}. However, E_{eff} and η_{eff} levels may also increase detrimentally. There is no mechanistic guideline dictating the particle sizes and types that would result in optimum properties. Here, we propose a numerical optimization method, first by generating microstructures with a Monte-Carlo-based (i.e. random generation) algorithm, and then predicting their effective properties.

Two major categories for particle mixing algorithms are available in the literature: (a) collective rearrangement (i.e. simultaneous updating of particle size and/or location with the assumption of a binding forcefield) and (b) sequential addition (i.e. particles are added one by one). The former is computationally very expensive and inherently limited to N $<10^3$ [5]. The latter is computationally more efficient [6]. We utilize a previously developed sequential Monte-Carlo algorithm [1] to generate various TIM structures to study their effective properties as a function of particle size distribution and determine the optimal structure.

MODEL DESCRIPTION

Generation of structure via Monte-Carlo algorithm

In this method, that we outlined in detail in our earlier publication [1], three types of particles are packed by randomly generating their type, size and location within a constant-volume space with non-periodic boundary conditions.

We adopt a sequential packing approach to ensure the maximum utilization of the available interstitial space. This recipe was conditioned to pack the largest particles first (up to total volume fraction of 25%), followed by second largest ones (up to 35% of total volume fraction) and the smallest one to a total particle volume fraction of 50% in the box. We note that the 50% total volume fraction is not the saturation state; however, for the current paper, we attempt to identify the optimized filler size ranges before proceeding to saturated volume fractions in a future study.

Inter-particle heat/force transfer models

To determine k_{eff} of discrete particulate composites, we utilize the recently revisited analytical framework of inter-particle thermal conduction [7] by Dan et al., which was originally derived by Batchelor and O'Brien [8]. They assumed that confronting hemispherical portions of respective particles take part in heat/force exchange (Fig. 2) via a cylindrical conduit [9] whose radius r_{ij} is given by [10]:

$$r_{ij} = \alpha \frac{2 r_i r_j}{r_i + r_j} \tag{1}$$

where α is a tuning parameter whose value is determined by benchmarking simulation results with experimental data (described in forthcoming section). The inter-particle thermal resistance, R_{ij} (°C/W) is computed by linearly summing intra-particle (R_i and R_j) and trans-matrix (R_m) resistances [8].

Subbarayan and co-workers demonstrated that the same analytical expressions could be utilized for force exchange [9]. The inter-particle compliance ($1/E_{ij}$) can then be obtained by summing matrix and individual particle compliances ($1/E_m$, $1/E_i$ and $1/E_j$ respectively). The readers are referred to the authors' earlier publication for full details [1].

3D network of heat/force transfer

The collection of particles forms a 3D global network (Fig. 2), through which heat/force is transported. The condition for constructing this network is that a particle i interacts with its neighbor j if [10]:

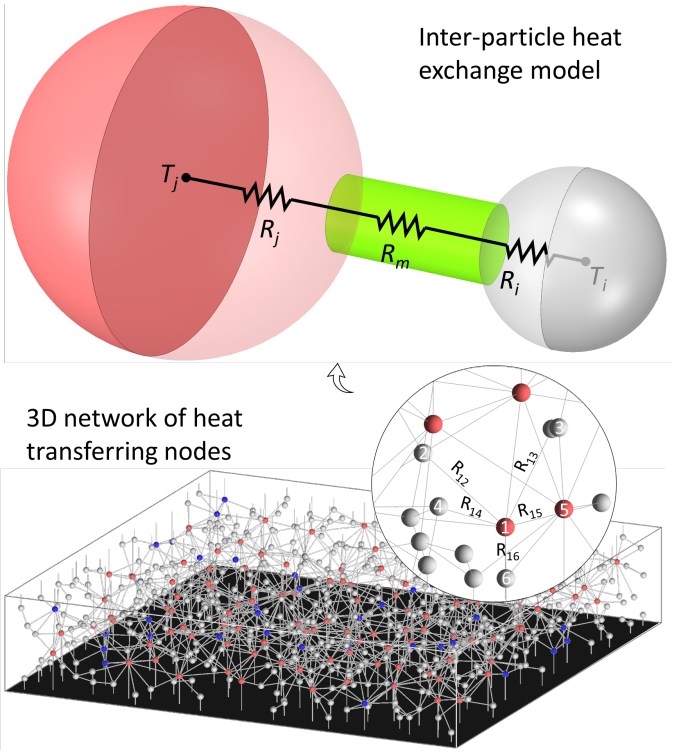

Fig. 2 (Top) model for inter-particle heat exchange with three thermal resistance terms. (Bottom) 3D network of thermal resistances, each line representing R_{ij}.

$$h_{ij} < \varepsilon \frac{2 r_i r_j}{r_i + r_j} \tag{2}$$

where h_{ij} is the minimum particle-to-particle surface distance and ε is another tuning parameter signifying the degree of inter-particle connectivity. Its value is determined from comparing simulation results with experimental data (described in next section).

Prediction of k_{eff} and E_{eff}

Heat (Q_{total}) is assumed to flow from the bottom to the top boundary with adiabatic sidewalls. At any node i connected to its neighbors j (where, j = 1,2,3… $N_{neighbor}$), the steady-state heat/force inflow must equal heat/force outflow [11]. Thus, one can write:

$$\sum_{j=1}^{N_{neighbor}} Q_{ij} = T_i\left(-\sum_{j=1}^{N_{neighbor}} \frac{1}{R_{ij}}\right) + \sum_{j=1}^{N_{neighbor}} \frac{T_j}{R_{ij}} = 0 \tag{3}$$

By ascribing the boundary conditions (for example, T_{top} = 0 and T_{bottom} = 1) one can solve for all the nodal temperatures (T_i) within the bulk of the material. For the force model, T_i terms are replaced by displacement terms (u_i) and resistances R_{ij} replaced by compliance ($1/E_{ij}$) in Equation (3). Then, the total heat (Q_{total}) or total force (F_{total}) flux can be computed considering the particles directly in contact with the either boundary. Finally, k_{eff} and E_{eff} can be computed as follows:

$$k_{eff} = \frac{Q_{total}}{T_{bottom} - T_{top}} \frac{L}{A};\ E_{eff} = \frac{F_{total}}{u_{bottom} - u_{top}} \frac{L}{A} \tag{4}$$

where A and L are area and thickness of the TIM respectively.

The model is validated by tuning the parameters α and ε, so that they can reproduce experimentally determined effective properties of a representative TIM. This set of values are calibrated to reproduce the empirically-determined k_{eff} and E_{eff} levels of the representative TIM with an error <0.3%. These values are used for subsequent structures generated through the packing algorithm. The η_{eff} model (outlined below) does not require any calibration. For the heat transport model, we have determined the values of α and ε to be 1.5 and 1.73 respectively. For the force balance model, they are 1.5 and 1.35 respectively. A sensitivity analysis of the predicted properties with α and ε will be discussed in the next section.

η_{eff} Model

We use a discrete η_{eff} model accounting for the polydispersity of particle aggregate proposed by Dörr et al. [12]. For a N-disperse composite material, where each particle is added sequentially, the η_{eff} can be expressed as [12]:

$$\frac{\eta_{eff}}{\eta_m} = \prod_{i=1}^{N}\left[\left(2.5 - \frac{2}{\Phi_i}\right)\Delta\phi_i + \left(5.2 - \frac{3}{\Phi_i^2}\right)(\Delta\phi_i)^2 + \left(1 - \frac{\Delta\phi_i}{\Phi_i}\right)^{-2}\right] \tag{5}$$

For i > 1, the maximum volume fraction achievable, Φ_i can be computed from the following expression:

$$\Phi_i = \Phi_{i-1}\sum_{j=1}^{i}\Delta\phi_j\left(\Phi_{i-1}\Delta\phi_i + \sum_{j=1}^{i-1}\Delta\phi_j\right)^{-1} \tag{6}$$

Note that for monodisperse distribution (when i = 1), theoretical limit of the maximum volume fraction, $\Phi_1 = 0.64$ [10, 13]. The infinitesimal volume fraction increment (with respect to the available space) $\Delta\phi_i$ can be expressed [12] as:

$$\Delta\phi_i = \phi_i\left(1 - \sum_{j=i+1}^{N}\phi_j\right)^{-1} \tag{7}$$

Where, ϕ_i is the volume fraction of the i-th particle with respect to the entire TIM volume.

Determination of optimum computational domain size

To determine the computational volume size, we consider a mono-disperse system with a fixed TIM thickness. We gradually increase the volume size by increasing the lateral dimensions until a saturation is reached in terms of the predicted volume fraction (63-64%) and effective properties (k_{eff} and E_{eff}). This procedure was repeated for several particle sizes that were 5%, 25%, 50% and 75% of the fixed TIM thickness. The lateral sides of the volume (which yields size-independent properties) are found to be about 7 times the mean diameter of the largest particle type for the fixed TIM thickness.

RESULTS & DISCUSSION

TIM structures with systematic variation in filler size

To begin our discussion, we first generate eighteen cases of three-filler (labeled A, B and C) particulate composites by systematically varying one particle size at a time. We generate all these structures up to a volume fraction of 50% within a constant representative volume element, which ensures no size-dependent simulation artefacts. The structures are presented in Fig. 3. For ease of visualization, all volumes are sliced into equal cubes although the lateral dimensions of the computational volumes were set at ~7X the largest particle size. The size distribution functions of individual filler types are assumed Gaussian with pre-defined means (μ_A, μ_B and μ_C) and standard deviations (σ_A, σ_B and σ_C). While packing, each particle is selected from the three-sigma interval around the mean. The standard deviations of these distribution are 8.57% of the average diameter of the smallest particle type (i.e. the one designated as type C).

In Fig. 3, for the first set of cases (CASE 1 through 6), the size of the largest filler A is gradually increased from a value close to the diameter of the medium-sized filler B. Sizes of the fillers B and C are kept constant. For the second set of cases (CASE 7 through 12), filler B size is systematically varied between the smallest C and the largest filler A sizes. For the last set of cases (CASE 13 through 18), the smallest filler size C is varied up to a value close to the medium sized filler B, while the sizes of A and B are kept constant. We predict effective properties of all these structures as presented in Fig. 4.

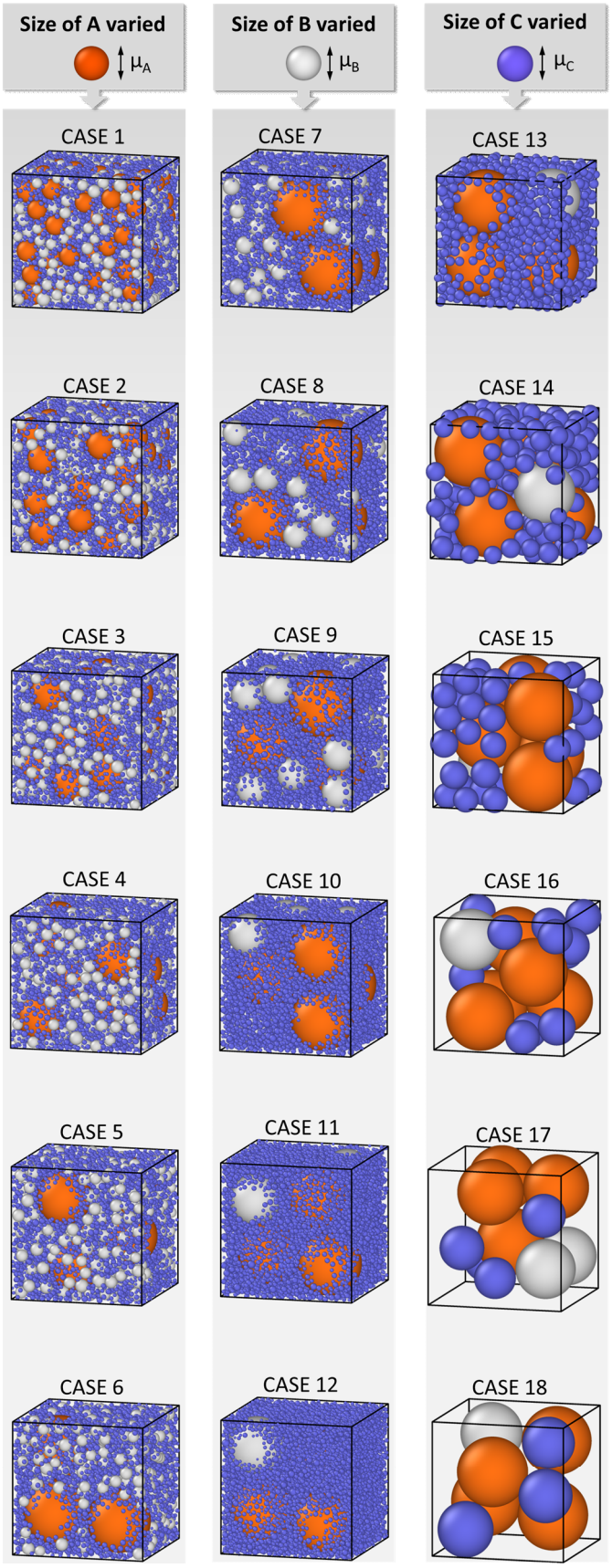

Fig. 3 Various cases of filler packing: sizes of fillers A, B and C are respectively varied in CASEs 1-6, 7-12 and 13-18.

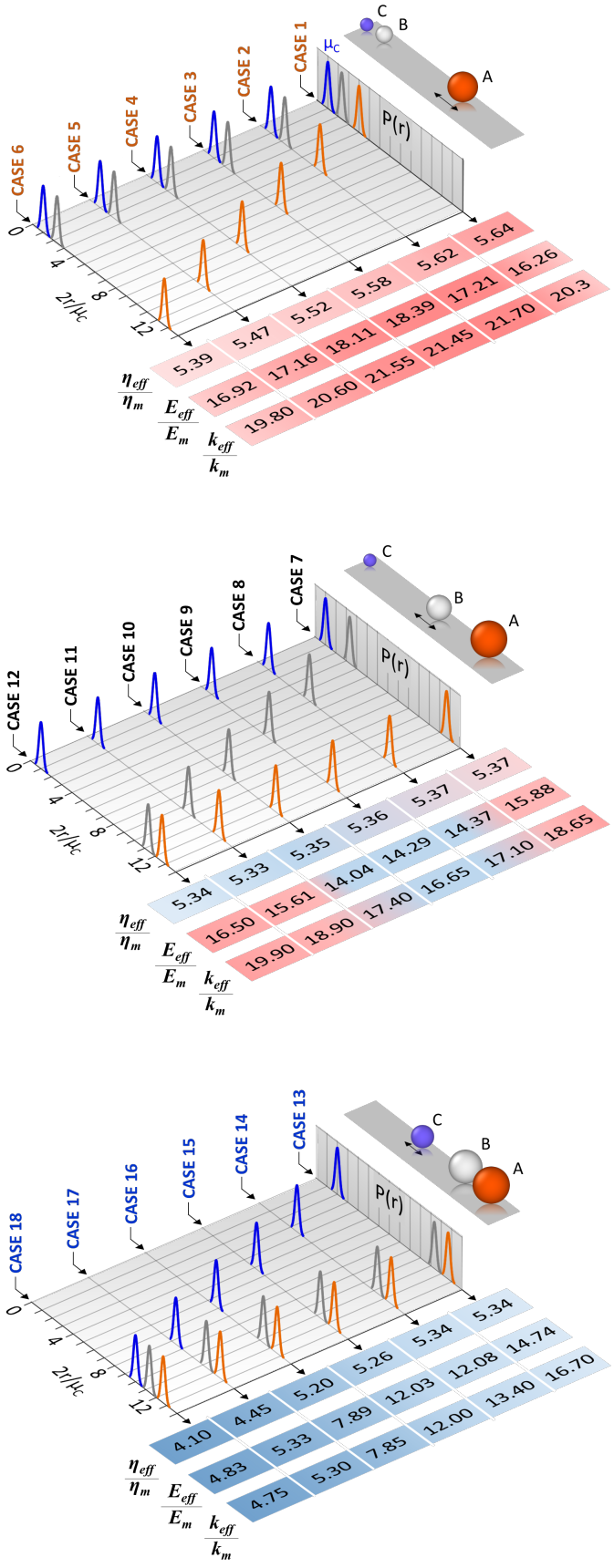

Fig. 4 Predicted effective properties for various filler sizes (normalized by smallest mean diameter of type C, μ_C).

Size distribution-dependent effective properties

We assign different sets of properties to each particle type (Table 1), where the two largest filler types (A and B) are considered to be of the same material.

Table 1. Filler properties used in the simulations.

	Thermal conductivity, k_p/k_m	Elastic modulus, E_p/E_m
Filler A	1025	69×10^6
Filler B	1025	69×10^6
Filler C	125	370×10^6

It is important to note that the current model is generic, and one can ascribe any realistic material properties to these fillers. Using these properties, we predict effective properties of all the generated cases. The predicted results normalized to the matrix properties are presented in Fig. 4. From Fig. 4, the maximum level of k_{eff} is achieved in CASE 2, CASE 3 and CASE 4, where it is increased by about 20-21 times the matrix conductivity k_m. Noticeably, degradation in viscosity and compliance levels are not significant among these cases. Thus, enhancement of thermal conductivity should be directed towards further fine-tuning in the narrow range between CASE 2 and CASE 4. In general, the combinations of large particles and very small particles (CASE 1 through 6), where the largest particles size are about 5-10 times the smaller particle size, have better thermal conductivities. In future work, we will refine this range by running the simulations to saturated particle volume fractions.

The reason could be attributed to the fact that the smaller particles are able to fill in the interstitial gap among the relatively larger ones in these structures. These small particles provide greater degree of heat transport path because of the increase in the surface area, whereby the total proportion of the matrix transporting the heat is reduced. By contrast, the minimum enhancement of thermal conductivity is noted for CASE 13 through 18, where the volume is filled with progressively large particles, which leaves more interstitial gap among them. This is particularly so since the particles are assumed perfectly spherical. Thus, two confronting spheres will have more matrix material between them in comparison with two flat heat-transmitting facades. For the cases with reduced k_{eff}, the average interstitial gap among the particles is substantial. In such case, heat would be transported by a significant portion of the matrix material. This rationale could be extended to explain why k_{eff} is increased in CASE 12.

A similar trend in the structure-property correlation is noted in E_{eff} levels across cases since the spring model considers force transfer mechanism to be analogous to heat transport. The same rationale as described above for the trends in k_{eff} and various structures could be applied to comprehend these trends in E_{eff}. On the other hand, from the viscosity model, we note that the variation in η_{eff} is insubstantial for CASE 1 through 12. It decreases monotonically from CASE 1 through CASE 18. Notice that the decrease in η_{eff} with respect to variation in the largest particle size (CASE 1 through 6) is insignificant compared to the variation in the smallest particle size (CASE 13 through 18).

We also present a study on the sensitivity of the tuning parameters (α and ε) with respect to k_{eff} in Fig. 5. It follows that the variation in the effective thermal conductivity is linear with each parameter. Here, when each parameter is changed, the other one was kept constant. The currently used values are indicated with arrows. The values of these parameters are determined by (a) first, determining material type and filler size distribution of an actual benchmark TIM material with known effective properties, (b) then, simulating its micro-structure in terms of particle type and size distribution, and finally solving for α and ε values which reproduce the known properties (k_{eff} and E_{eff}) of the benchmark TIM with error level < 0.1%. As Fig. 5 suggests, 10% of deviation in the currently chosen α and ε values causes a ~10% change in k_{eff} levels. We use thus-obtained magnitudes to predict effective properties of other simulated TIM structures.

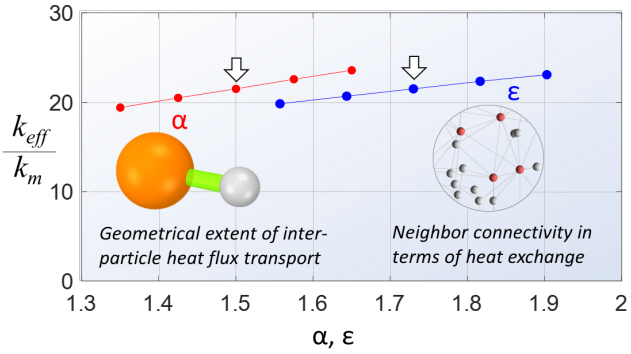

Fig. 5 Study of tuning parameters (α and ε) sensitivity on k_{eff} (arrows indicating currently chosen values). α is used to regulate exposure level of thermal flux (i.e. diameter of heat conduit) between confronting hemispheres, while ε to adjust extent of thermal neighborhood (i.e. number of neighboring particles,) of a certain particle.

The current modeling results provide a physical rationale why some cases (specifically with prevalent small particles) have better thermal conductivity. It is related to how thermal path is established by the optimum combination of large and very small particles. For instance, a particulate structure would have superior heat transport capability if the smallest particles fill in the interstitial gap among the largest ones to effectively establish enhanced thermal paths. It should also be noted that the heat transport could occur along multiple parallel paths if thermal resistances for respective paths are of equal or comparable magnitudes. For instance, if there is an interposing smaller particle between two large particles, the two large particles may establish a direct thermal path and a parallel path could also exist connecting the large particles with the smaller interposing particle. The discrete nature of the thermal resistance network accounts for this physics. If multiple parallel paths of heat are physically possible, as dictated by the condition in Equation (2), the appropriate network would be established and the nodal temperature solutions (hence, the

effective conductivity) would be adjusted accordingly. This scenario is physically possible in nature.

CONCLUSIONS

With a previously-developed algorithm, we have generated computational models of TIM structures by systematically varying sizes of three different particle types. We have also utilized analytical models from literature to predict k_{eff}, E_{eff} and η_{eff} for all these structures to reveal the dependency of effective properties on the fillers sizes while keeping the other attributes of the constituent materials (i.e. number of filler types and the type of the matrix) constant.

We find that the lateral dimensions of the computational volume for the packing algorithm should be about 7 times the largest particle size for a fixed TIM thickness. The results quantitatively establish an optimum window of filler size distributions for optimal properties, i.e. the largest particle size should be about 5-10 times the smallest particle size. Further refinement of this range will be studied in future work. The main contribution of the current research is to provide promising physical guidelines for optimizing TIMs. In addition, the modeling framework paves the way for studying roles of different chemical species as filler types and matrix materials in the future.

ACKNOWLEDGEMENTS

The authors gratefully acknowledge the support of Arvind Kumar, Leland Chang, Jeff Burns, Rama Divakaruni, Dinesh Gupta and Sushumna Iruvanti from IBM.

REFERENCES

[1] P. Chowdhury, K. Sikka, A. De Silva, and I. Seshadri, "On Thermal Interface Materials With Polydisperse Fillers: Packing Algorithm and Effective Properties," in *ASME 2018 International Technical Conference and Exhibition on Packaging and Integration of Electronic and Photonic Microsystems*, 2018, p. V001T01A007–V001T01A007.

[2] K. Pietrak and T. S. Wiśniewski, "A review of models for effective thermal conductivity of composite materials," *J. Power Technol.*, vol. 95, no. 1, pp. 14–24, 2014.

[3] A. Bar-Cohen, K. Matin, and S. Narumanchi, "Nanothermal interface materials: technology review and recent results," *J. Electron. Packag.*, vol. 137, no. 4, p. 040803, 2015.

[4] R. Prasher, "Thermal interface materials: historical perspective, status, and future directions," *Proc. IEEE*, vol. 94, no. 8, pp. 1571–1586, 2006.

[5] B. D. Lubachevsky and F. H. Stillinger, "Geometric properties of random disk packings," *J. Stat. Phys.*, vol. 60, no. 5–6, pp. 561–583, 1990.

[6] E. Santiso and E. A. MÜLLER, "Dense packing of binary and polydisperse hard spheres," *Mol. Phys.*, vol. 100, no. 15, pp. 2461–2469, 2002.

[7] B. Dan, S. Kanuparthi, G. Subbarayan, and B. G. Sammakia, "An Improved Network Model for Determining the Effective Thermal Conductivity of Particulate Thermal Interface Materials," in *ASME 2009 InterPACK Conference collocated with the ASME 2009 Summer Heat Transfer Conference and the ASME 2009 3rd International Conference on Energy Sustainability*, 2009, pp. 69–81.

[8] G. K. Batchelor and R. W. O'Brien, "Thermal or electrical conduction through a granular material," *Proc R Soc Lond A*, vol. 355, no. 1682, pp. 313–333, 1977.

[9] P. K. Vaitheeswaran and G. Subbarayan, "Estimation of Effective Thermal and Mechanical Properties of Particulate Thermal Interface Materials (TIMs) by a Random Network Model," in *ASME 2017 International Technical Conference and Exhibition on Packaging and Integration of Electronic and Photonic Microsystems collocated with the ASME 2017 Conference on Information Storage and Processing Systems*, 2017, p. V001T02A020–V001T02A020.

[10] T. S. Yun and T. M. Evans, "Three-dimensional random network model for thermal conductivity in particulate materials," *Comput. Geotech.*, vol. 37, no. 7–8, pp. 991–998, 2010.

[11] K. K. Bodla, J. Y. Murthy, and S. V. Garimella, "Resistance network-based thermal conductivity model for metal foams," *Comput. Mater. Sci.*, vol. 50, no. 2, pp. 622–632, 2010.

[12] A. Dörr, A. Sadiki, and A. Mehdizadeh, "A discrete model for the apparent viscosity of polydisperse suspensions including maximum packing fraction," *J. Rheol.*, vol. 57, no. 3, pp. 743–765, 2013.

[13] D. Quemada, "Rheology of concentrated disperse systems and minimum energy dissipation principle," *Rheol. Acta*, vol. 16, no. 1, pp. 82–94, 1977.